TECHNICAL REPORT

19TH INTERNATIONAL SYMPOSIUM ON LASER-AIDED PLASMA DIAGNOSTICS
22–26 SEPTEMBER, 2019
WHITEFISH, MONTANA, U.S.A.

Bench test of microwave imaging reflectometry system for EAST tokamak

W. Liao,[a] **F.X. Gao,**[a] **C.M. Qu,**[a] **X.H. Xu,**[a] **L.F. Zhang,**[a] **Z.H. Li,**[a] **S.C. Yang,**[a] **C.W. Domier,**[b] **Y.L. Zhu,**[b] **G. Zhuang,**[a] **W. Liu,**[a] **N.C. Luhmann Jr.**[b] **and J. Xie**[a]

[a] *School of Physical Sciences, University of Science and Technology of China,*
  Hefei, Anhui 230026, China

[b] *University of California,*
  Davis, California 95616, U.S.A.

  E-mail: jlxie@ustc.edu.cn

ABSTRACT: Microwave Imaging Reflectometry (MIR) has been developed for measuring two-dimensional electron density fluctuations on many Tokamaks. A MIR system with 96 pixels (12 poloidal × 8 radial) has been fabricated for EAST tokamak. In the paper, we present the evaluation results in laboratory bench test with details, including performance of the electronic system and optics. With an artificial target as the real plasma cutoff layer, it has been proved that the EAST MIR system has the capability to reconstruct the correct corrugated shape of cutoff layer.

KEYWORDS: Plasma diagnostics - interferometry, spectroscopy and imaging; Plasma diagnostics - high speed photography

---

[1]Corresponding author.

Contents

1 Introduction

Microwave reflectometer has been widely used for density fluctuation measurements on Tokamak devices. Launching a probe beam with fixed frequency f_0, the phase variation $\delta\phi$ of the reflected signal will carry the density fluctuation information at the location where the cutoff frequency equal to f_0. For ideal case, when the cutoff layer is flat, there has a simple relation that phase variation is proportional to the density fluctuation, $\delta\phi \propto \tilde{n}_e/n_e$. Considering the real plasma case, the cutoff layer is actually corrugated with the turbulence developed on it. The probe beam will be scattered back on the corrugated surface, which may cause serious interference pattern in the detection location. Thus the conventional reflectometers with small aperture collecting optics are not able to collect enough scattered signals to reconstruct the real phase on the cutoff layer. The simple relation between phase variation and density fluctuation is broken. Therefore collecting optics with large aperture are highly recommended in microwave reflectometry in order to interpret data correctly [1]. Then it is natural to expand the single detector to 1D receiver detector array and increase the number of probing frequencies, which is the origin of the Microwave Imaging Reflectometry (MIR). As a promising tool to visualize 2D density fluctuation, MIR diagnostic system has been applied in DIII-D [2], KSTAR [3] and LHD [4].

A new MIR system has been built for EAST tokamak. In this paper, we will present the bench test of the whole system, including the performance evaluation of the IF electronics system and the imaging property of whole MIR system.

2 EAST MIR system

EAST MIR system utilizes X-mode polarized probe beam to illuminate the observed area while a 12-channel detector array is employed to receive signals reflected by 12 different poloidal position. The probe beam contains eight frequencies corresponding to eight radial positions, while the
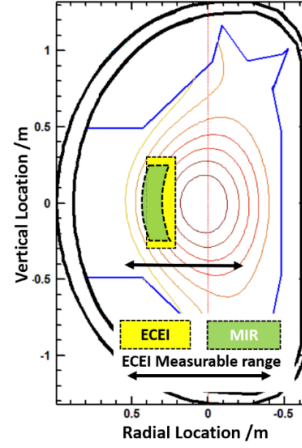
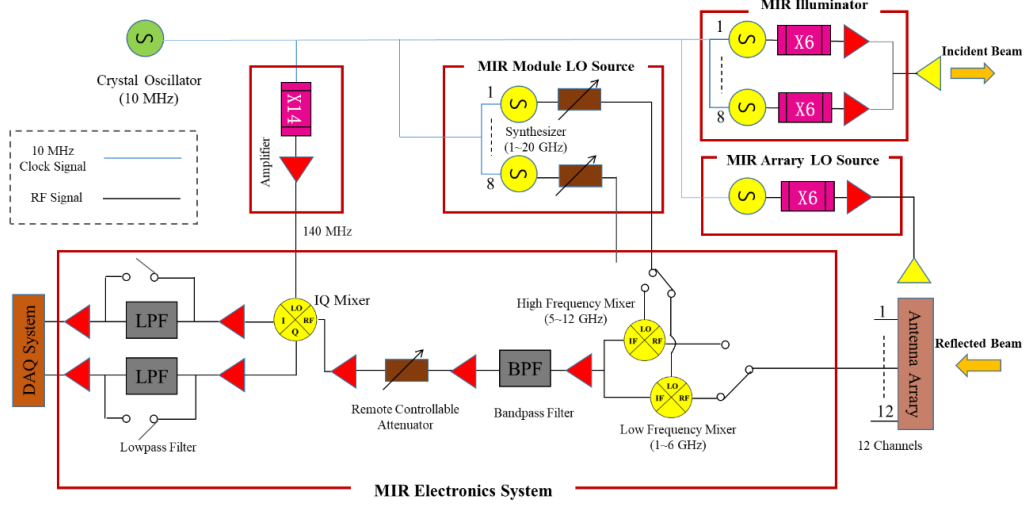**Figure 1**. Observe area of EAST MIR system and EAST ECEI system.

Figure 2. Schematic of EAST MIR system.

frequencies can be tuned independently over 75 GHz ~ 105 GHz. For typical discharge of EAST plasma, MIR system with 96 pixels (12×8) is able to cover a wide radial range ($r/a = 0.41 \sim 0.99$). Together with the installed ECE Imaging system [5] co-located in the same port, the evolutions of the electron density and temperature fluctuations will be simultaneously obtained in the same observation area, shown in figure 1.

In order to obtain phase information from reflected RF signals with multi-frequency, a two-step-down-conversion system is employed to implement frequency selection and phase detection. The schematics of EAST MIR system is shown in figure 2, which contains five major parts: illuminator, array LO source, module LO source, antenna array and electronic system. Each frequency component of probing beam is generated by multiplying the output signal of one synthesizer. A power combiner merges eight components into one. Launched by a high gain pyramid horn, the combined signal propagates through the transmitting optics where the curvature of the probe beam is modified to match the shape of cutoff layer.
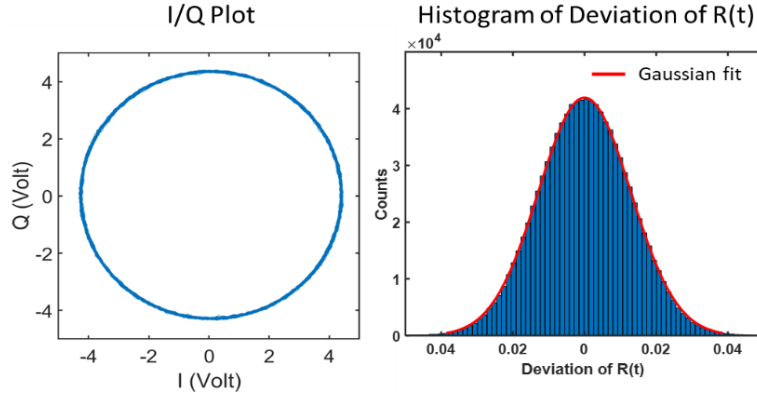
Figure 3. a) IQ plot; b) histogram of centralized $R(t)$ and Gaussian fit results.

After the illumination signal is reflected, each frequency component will carry the density fluctuation information of cutoff layers at corresponding radial locations. These reflected signals are collected via receiving optics and projected onto the Schottky diode detector array. The array LO signals is also projected onto the detector array and mixed with the reflected signals to complete the first down-conversion. It should be noted that here double sideband mixer process is applied, not like the single sideband system using in ECE Imaging.

The IF signal generated by each detector in antenna array still contains eight different frequencies, carrying information from same poloidal position but different radial positions in the observation area. The second step of down conversion is needed to achieve frequency selection. The IF signal from each detector is divided into eight branches, and each branch is mixed with the output of one module LO source. The frequency of module LO source is determined by the frequencies of illuminator and array LO. Selectable dual mixer units are designed to expand the bandwidth of electronic system to 12 GHz with reasonable cost. Band pass filter with 20 MHz bandwidth is followed by the mixer. With deliberately setting the frequencies of illuminator, array LO and module LO, only one frequency component will pass through the filter while other components are rejected. Finally, the signal is inputted into IQ mixer together with a 140 MHz LO signal, then the phase variation at one pixel is obtained.

3 Evaluation of electronic system performance

3.1 IQ signal imbalance

In IQ phase detection, the imbalance of in-phase (I) and quadrature (Q) signal is a major performance-limiting issue. There are two major causes, DC offset and amplitude imbalance. IQ signal with imbalances can be represented as equation (3.1) and (3.2):

$$I(t) = I_0 + A_I \sin(\omega t) \tag{3.1}$$

$$Q(t) = Q_0 + A_Q \cos(\omega t) \tag{3.2}$$

I_0 and Q_0 represent DC offsets of IQ signals while A_I and A_Q means amplitudes of IQ signal. To measure the imbalance of IQ signals, pure sinusoidal wave from synthesizer is provided as input of MIR electronic system and the frequencies of IQ signals is set at 10 kHz. The IQ outputs are
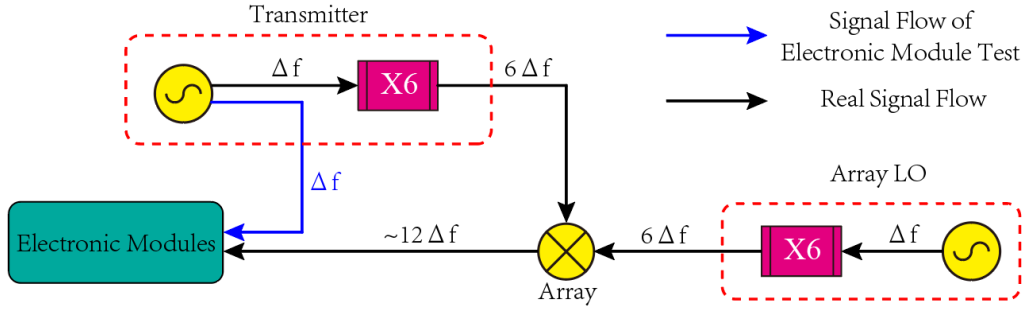
Figure 4. Schematics of the phase noise evaluation for simplified case and real case.

acquired using digitizer with 1MS/s sample rate for a period of several seconds. Since the average values of the sinusoid terms can be ignored, the DC offsets I_0 and Q_0 equal to the mean value of $I(t)$ and $Q(t)$ over whole sample time. The DC offsets of in-phase and quadrature signal are 69.5 mV and 33.8 mV relatively.

For amplitude imbalance measurements, $R(t)$ is introduced as the radius of IQ plot, which is defined as shown in equation (3.3).

$$R(t) = \sqrt{(I(t) - I_0)^2 + (Q(t) - Q_0)^2} = \sqrt{A_I^2 \sin^2(\omega t) + A_Q^2 \cos^2(\omega t)} \quad (3.3)$$

According to equation (3.3), if $A_I = A_Q$, then the value of $R(t)$ will be a constant, otherwise it will vary with time. The histogram of $R(t)$ variations is shown in figure 3, it is clear shown that the distribution of centralized $R(t)$ perfectly matches the Gaussian distribution. The mean of Gaussian fit almost equals to 0mV proved that the amplitudes of in-phase and quadrature signal are equal to each other. Also the noise level of electronic system is estimated around 9 mV, since the standard deviation of $R(t)$ equals $\sqrt{2}$ times of noise level of electronic modules.

3.2 Phase noise

As a phase detection system, phase noise of the MIR electronic system has direct impact on the results. The phase noise is expressed as the fluctuation of phase signal in time domain. The schematic of evaluation process is shown in figure 4.

Similar as the setup of IQ imbalance estimation, the synthesizer output is directly inputted into the IF module, the phase result based on the IQ signal should be a constant. In this simplified case, the phase variation is very small, shown in figure 5 as blue curve.

In order to simulate the real case, another configuration is adopted shown in figure 4, labeled with the black arrow (real signal flow). The output of frequency multiplier in which the frequency of synthesizer output is multiplied six times is treated as the signal reflected from the cutoff layer. Together with the array LO input, they are projected on the detector diode. The mixed output is transmitted to the MIR IF module. In this "real" case, the phase variation is shown in figure 5 as yellow curve with a maximum value as high as 1.5 rad, which is roughly the same level as 12 times of phase fluctuation in simplified case (shown in figure 5 as red curve). The reason is that the 6× multiplier not only multiply the frequency, but also multiply the phase noise of the synthesizer.

It should be noticed that the level of phase fluctuations is rather big, but the phase variation changes very slowly with time. The spectral density of the phase deviation is shown in figure 6.
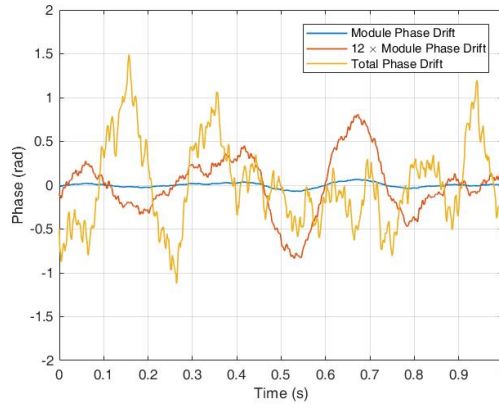
Figure 5. The time evolutions of the phase variations in two cases, blue curve is the simplified case and yellow curve is the real case.
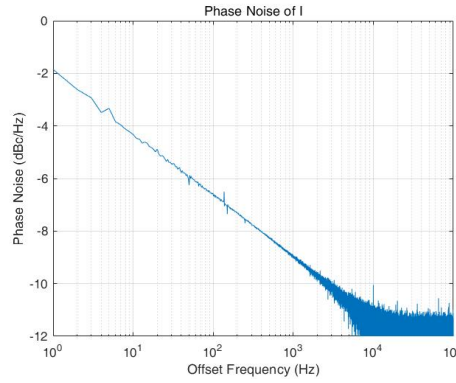

Figure 6. Spectral density of the phase deviation.

It is clearly shown that low frequency components dominate the phase noise, while in the relative high frequency region (> 1 kHz) the noise level is small. Fortunately, the high frequency part of the density fluctuation attracts more investigation in tokamak, thus the major part of phase noise can be removed by utilizing high pass filter in data processing.

4 Measurement using artificial target

The whole MIR system, including the optics and electronic system, are laid out in laboratory like the real situation. The sinusoidal corrugated metal surface of a wheel with curvature radius 450mm is used as artificial cutoff layer, shown in figure 7. The wavenumber of corrugation structure simulating poloidal rotating density fluctuation is $k_\theta = 0.42 \, \text{cm}^{-1}$ ($\lambda = 15 \, \text{cm}$). The peak-to-peak depth is about 3 mm, the double optical path difference 6 mm will result in a phase difference $\Delta\Phi \sim 4\pi$ rad for a 100 GHz probe beam.

The details of the EAST MIR optics have been given in our previous paper [6]. The optics has the capability to adjust the focus, zoom and field curvature. Both the illuminating optics and
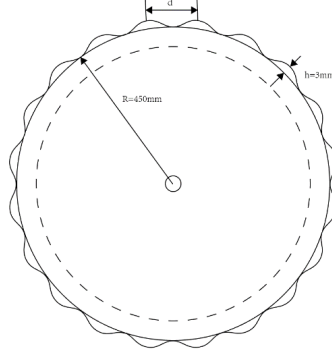
Figure 7. Geometric design of the artificial target: a wheel with radius 450 mm, the periodic structure on the metal surface with wavelength 15 cm and amplitude 3 mm.
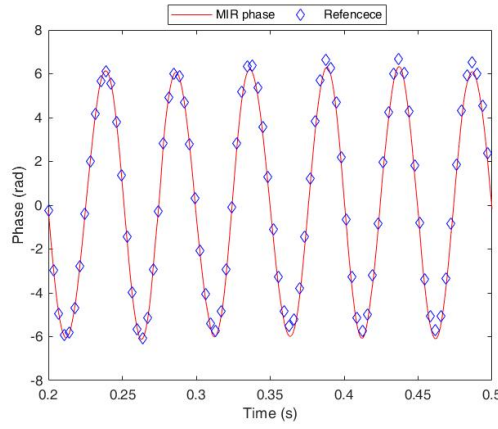

Figure 8. Comparison of observed phase (red curve, MIR phase)of one pixel and the expected phase (blue diamond, reference) variation due to the wheel rotation.

the collecting optics are carefully configured to achieve the match between the shape of wheel, the wave front of incident beam and the imaging layer of the antenna array.

Figure 8 shows the comparison between measured phase evolution of one MIR pixel and the expected phase induced by the radial variation of the corresponding observed location when the wheel is rotating. The coincidence result agrees well with the simple relation $\delta\phi \propto \tilde{n}_e/n_e$. In order to check the flexibility of the optics, two setups of collecting optics are tested with same focus position but different vertical observation range. The IQ outputs of 12 pixels at different vertical locations are acquired simultaneously and the surface shape are reconstructed to compare with the real geometrical shape. It is shown in figure 9 that MIR system gives correct shape in both narrow and wide cases.

5   Summary

The electronics system and optical system of EAST MIR have been tested, the offset of IQ signal imbalance is stable over sample time and the amplitudes of IQ signal are the same. The noise level of electronics system is about 9 mV. Also, the laboratory benchmark proved the ability of phase measurement of EAST MIR system and the flexibility of the optical system.
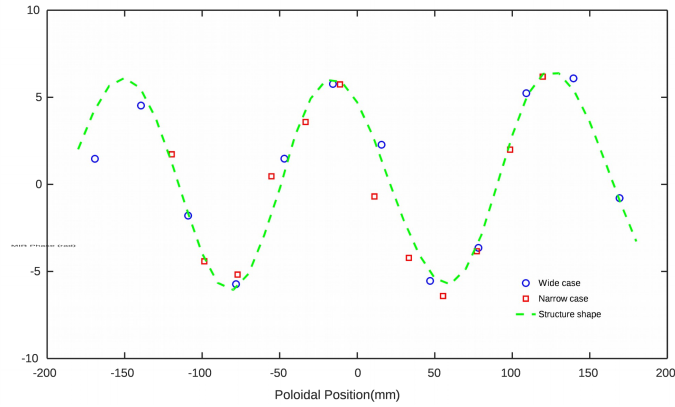
Figure 9. The reconstructed phase profile of the cutoff layer based on the MIR data (blue circles for the case with wide poloidal observation range, red squares for narrow range case), green dash line is the expected phase profile caused by the real structure on the metal surface.

Acknowledgments

References

[1] E. Mazzucato et al., *Fluctuation measurements in tokamaks with microwave imaging reflectometry*, *Phys. Plasmas* **9** (2002) 1955.

[2] C.M. Muscatello et al., *Technical overview of the millimeter-wave imaging reflectometer on the DIII-D tokamak*, *Rev. Sci. Instrum.* **85** (2014) 11D702.

[3] W. Lee et al., *Microwave imaging reflectometry for density fluctuation measurement on KSTAR*, *Nucl. Fus.* **54** (2014) 023012.

[4] S. Yamaguchi et al., *Microwave imaging reflectometry in LHD*, *Plasma Fus. Res.* **2** (2007) S1038.

[5] B.X. Gao et al., *The electron cyclotron emission imaging system on EAST with continuous large observation area*, 2002 *JINST* **13** P02009.

[6] Y.L. Zhu et al., *Millimeter-wave imaging diagnostics systems on the EAST tokamak*, *Rev. Sci. Instrum.* **87** (2016) 11D901.